# Long-term contamination of the Arabian Gulf as a result of hypothetic nuclear power plant accidents

**Vladimir Maderich, Roman Bezhenar, Ivan Kovalets, Oleksandr Khalchenkov, and Igor Brovchenko**

**Table. S1** List of meteorological stations used for verification of calculated precipitation intensities

| Country | Place name | Airport Code | Wmo code | latitude | longitude |
|---|---|---|---|---|---|
| Iran | Abadan | OIAA | 40831 | 30.377 | 48.215 |
| Saudi Arabia | Dammam | KFIA | 40415 | 26.433 | 49.8 |
| Saudi Arabia | Dhahran | OEDR | 40416 | 26.267 | 50.167 |
| Saudi Arabia | Al Ahsa | OEAH | 40420 | 25.3 | 49.483 |
| Iran | Bandar Lengeh | OIBL | 40883 | 26.528 | 54.828 |
| Iran | Bandar-E-Dayyer | - | 40872 | 27.833 | 51.933 |
| Iran | Bushehr | OIBB | 40858 | 28.963 | 50.819 |
| Iran | Kharg Island | - | 40845 | 29.267 | 50.267 |
| Qatar | Doha | OTBD | - | 25.273 | 51.608 |

**Table S2.** Total deposition on the surface of the Arabian Gulf calculated by RIMPUFF and DIPCOT atmospheric dispersion models for scenarios of accidents at Bushehr and Barakah NPP, described in paper; the relative difference between both estimates $R=100\%\cdot(Q_{RIMPUFF}-Q_{DIPCOT})/Q_{RIMPUFF}$ is presented in the last column.

| Accident Scenario | Radionuclide | Deposition on the Gulf, Bq (RIMPUFF) | Deposition on the Gulf, Bq DIPCOT | Relative Difference R, % |
|---|---|---|---|---|
| Bushehr | Cs-134 | 4.62E+16 | 4.55E+16 | 1.6 |
| Bushehr | Cs-137 | 9.25E+15 | 9.12E+15 | 1.4 |
| Bushehr | Ru-106 | 3.37E+16 | 3.57E+16 | -6.1 |
| Bushehr | Sr-90 | 3.13E+15 | 3.11E+15 | 0.68 |
| Barakah | Cs-134 | 4.36E+16 | 4.21E+16 | 3.4 |
| Barakah | Cs-137 | 2.43E+16 | 2.34E+16 | 3.7 |
| Barakah | Ru-106 | 7.30E+17 | 6.10E+17 | 16.4 |
| Barakah | Sr-90 | 6.10E+15 | 5.81E+15 | 4.8 |

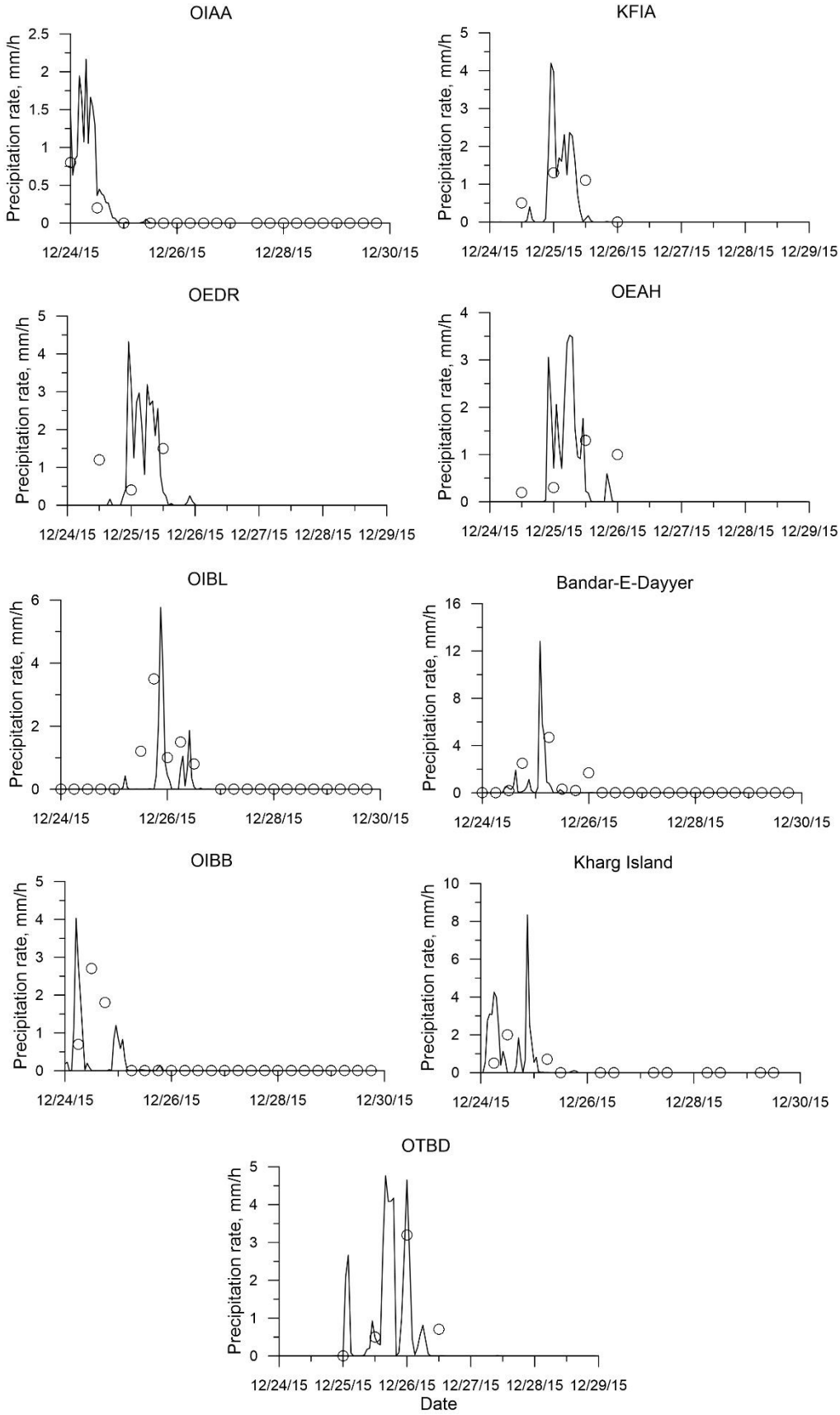


**Figure S1.** Precipitation intensities calculated by WRF (line) for the period 24-29 Dec 2015 compared with respective measurements (circles) extracted from Wolfram database https://reference.wolfram.com/language/ref/WeatherData.html

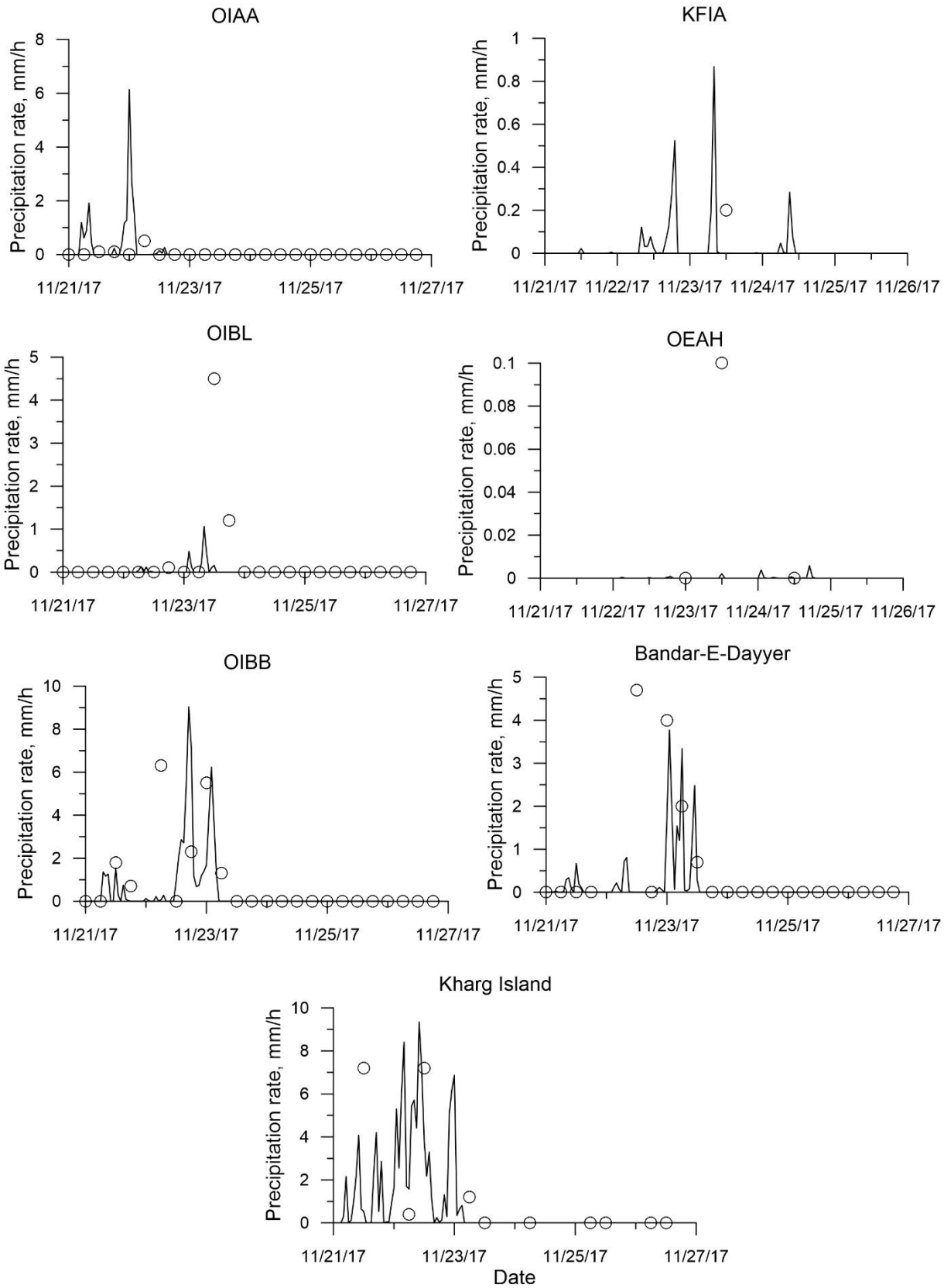


**Figure S2.** Precipitation intensities calculated by WRF (line) for the period 21-26 Nov 2017 compared with respective measurements (circles) extracted from Wolfram database https://reference.wolfram.com/language/ref/WeatherData.html

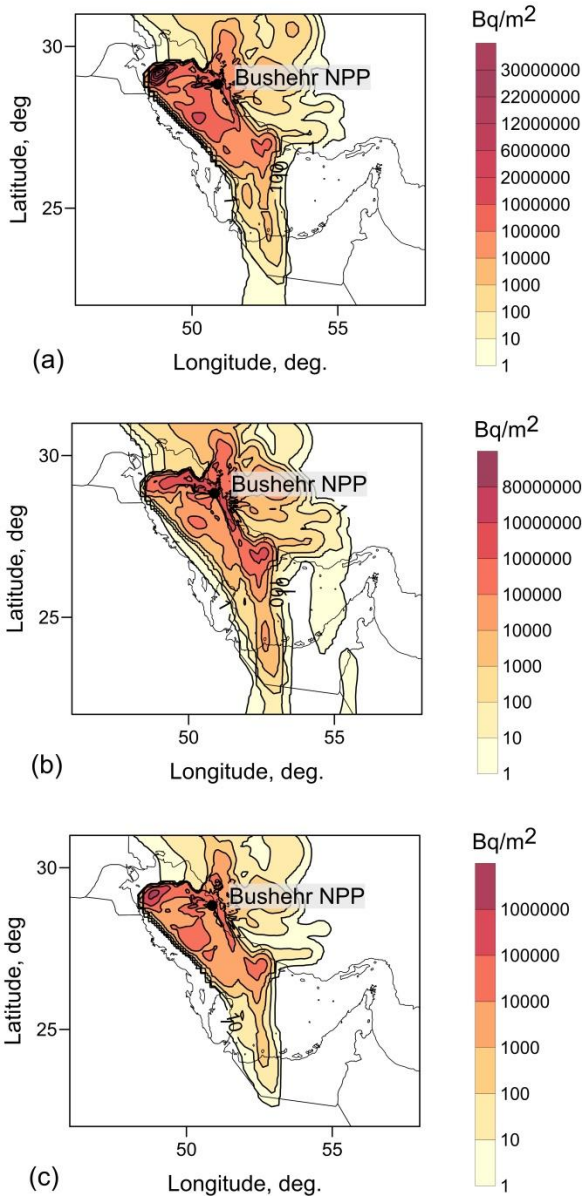


**Figure S3**. Maps of total (dry+wet) deposition density of **(a)** $^{134}$Cs, **(b)** $^{106}$Ru, **(c)** $^{90}$Sr simulated by JRODOS system for the hypothetical accident scenario at Bushehr NPP started on 24 Dec 2015, 08:00 h UTC; deposition maps are dated 96 h after the start of the accident scenario.

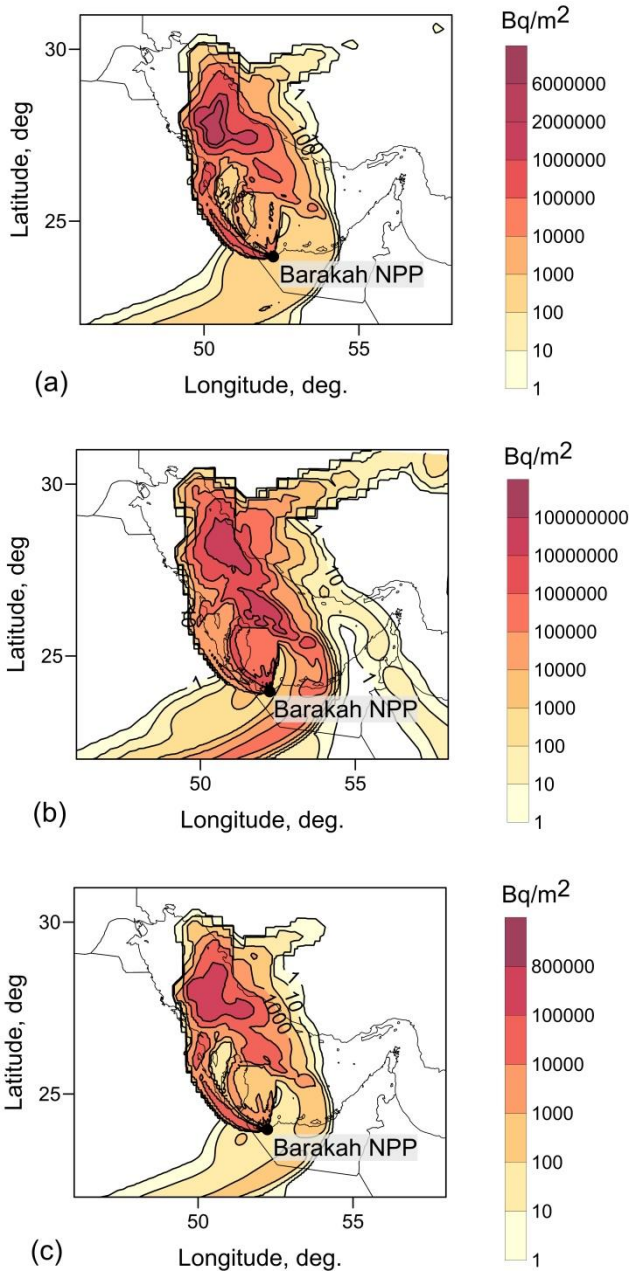


**Figure S4**. Maps of total (dry+wet) deposition density of **(a)** $^{134}$Cs, **(b)** $^{106}$Ru, **(c)** $^{90}$Sr simulated by JRODOS system for the hypothetical accident scenario at Barakah NPP started on 21 Nov 2017, 15:43 h UTC; deposition maps are dated 96 h after the start of the accident scenario.


**Figure S5**. Distribution of the $^{134}Cs$ concentration in water (Bq $m^{-3}$) at the Arabian Gulf surface after deposition for the hypothetical accident scenario at Bushehr NPP.

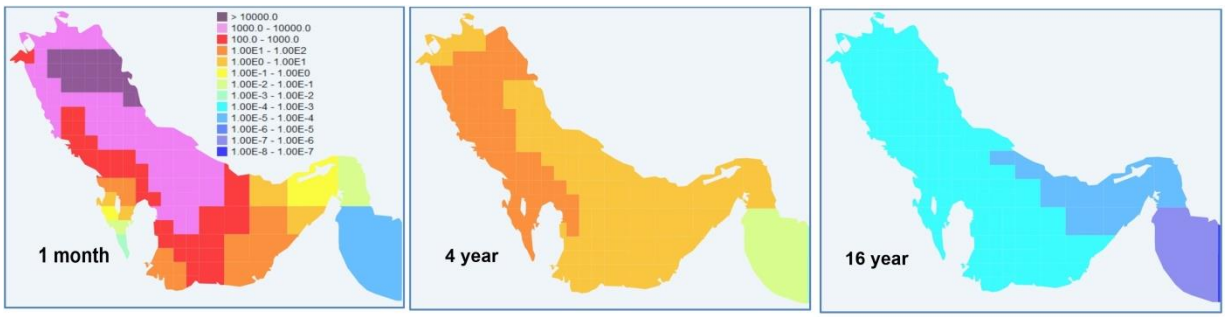


**Figure S6**. Distribution of the $^{106}Ru$ concentration in water (Bq $m^{-3}$) at the Arabian Gulf surface after deposition for the hypothetical accident scenario at Bushehr NPP.

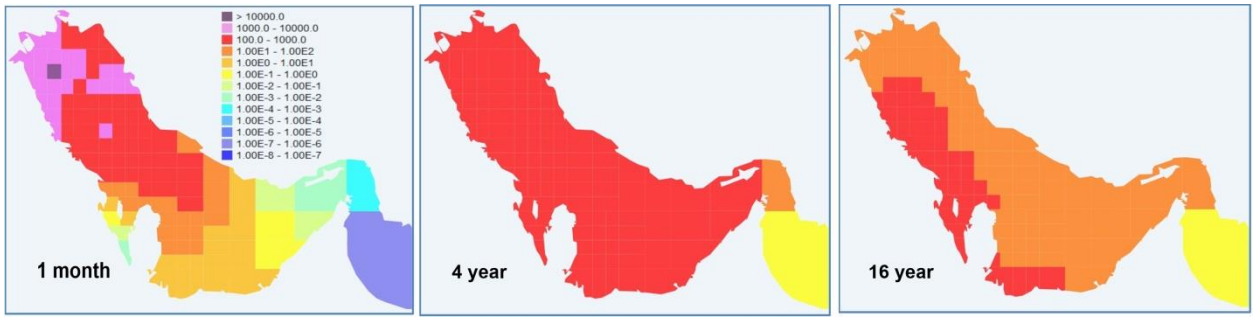


**Figure S7**. Distribution of the $^{90}Sr$ concentration in water (Bq $m^{-3}$) at the Arabian Gulf surface after deposition for the hypothetical accident scenario at Bushehr NPP.

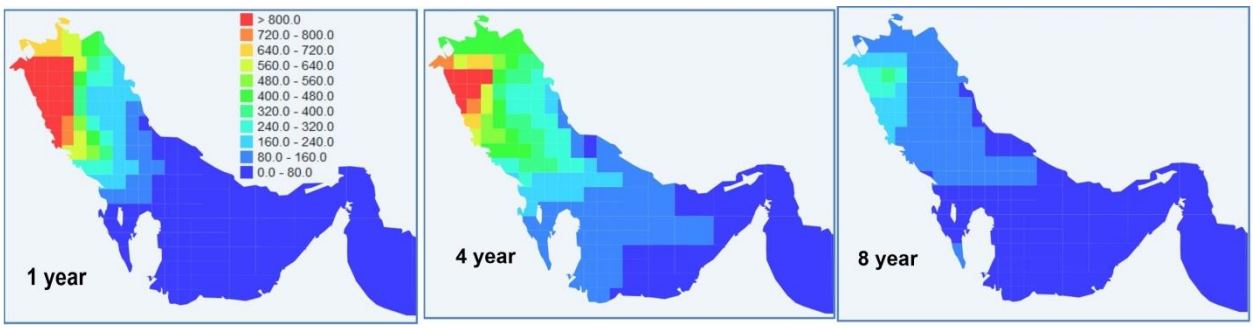


**Figure S8**. Distribution of the $^{134}Cs$ concentration in the upper layer of sediment (Bq $kg^{-1}$) at the Arabian Gulf surface after deposition for the hypothetical accident scenario at Bushehr NPP.


**Figure S9**. Distribution of the $^{106}Ru$ concentration in the upper layer of sediment (Bq $kg^{-1}$) at the Arabian Gulf surface after deposition for the hypothetical accident scenario at Bushehr NPP.

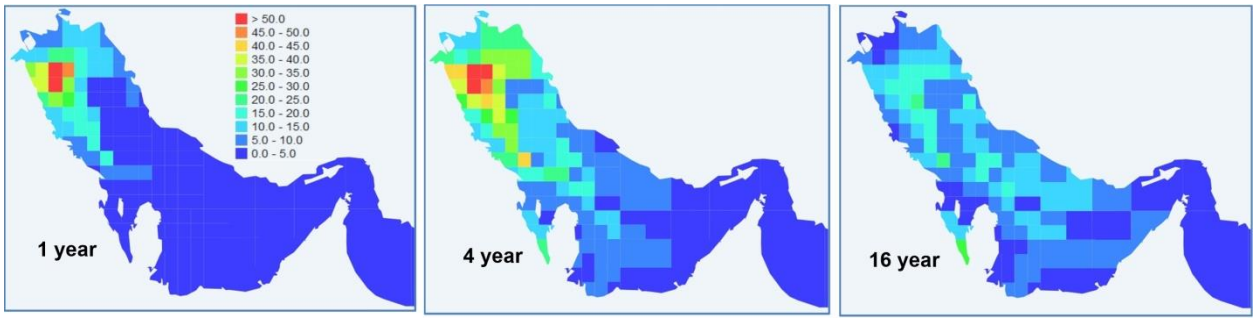


**Figure S10**. Distribution of the $^{90}Sr$ concentration in the upper layer of sediment (Bq $kg^{-1}$) at the Arabian Gulf surface after deposition for the hypothetical accident scenario at Bushehr NPP.

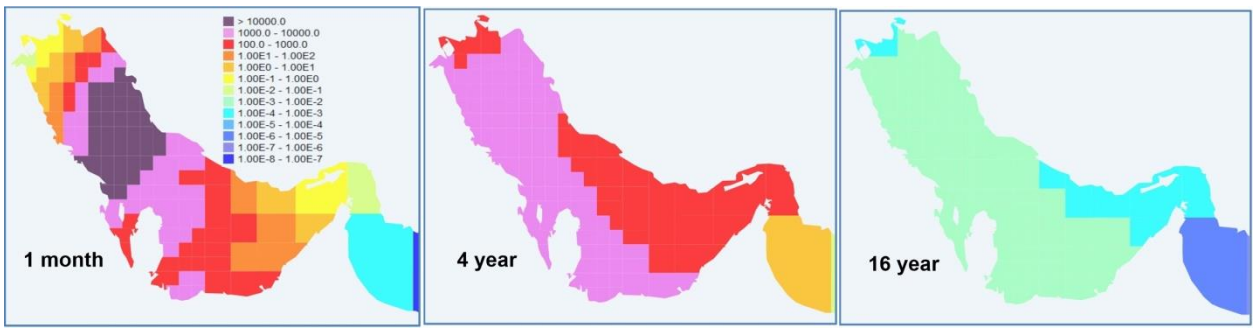


**Figure S11**. Distribution of the $^{134}Cs$ concentration in water (Bq $m^{-3}$) at the Arabian Gulf surface after deposition for the hypothetical accident scenario at Barakah NPP.

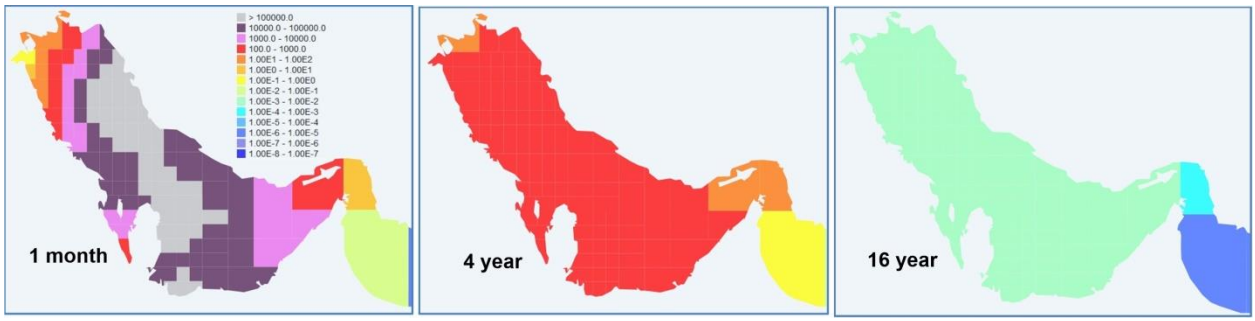


**Figure S12**. Distribution of the $^{106}Ru$ concentration in water (Bq $m^{-3}$) at the Arabian Gulf surface after deposition for the hypothetical accident scenario at Barakah NPP.

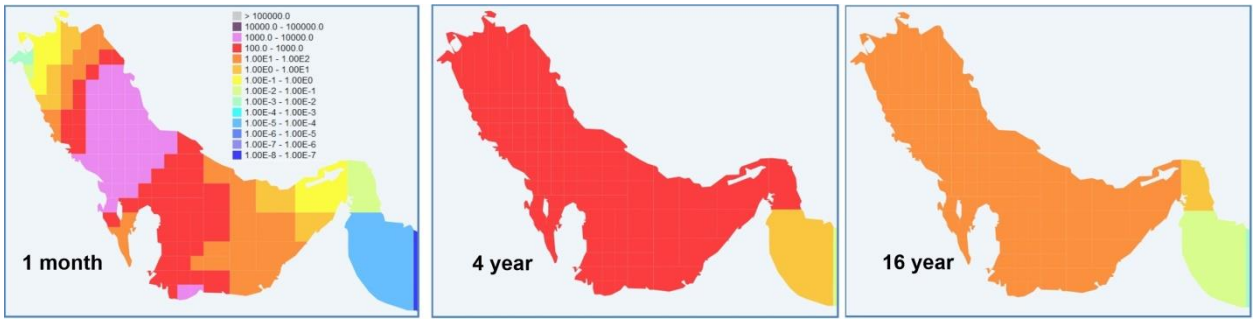


**Figure S13**. Distribution of the $^{90}Sr$ concentration in water (Bq $m^{-3}$) at the Arabian Gulf surface after deposition for the hypothetical accident scenario at Barakah NPP.


**Figure S14**. Distribution of the $^{134}Cs$ concentration in the upper layer of sediment (Bq kg$^{-1}$) at the Arabian Gulf surface after deposition for the hypothetical accident scenario at Barakah NPP.

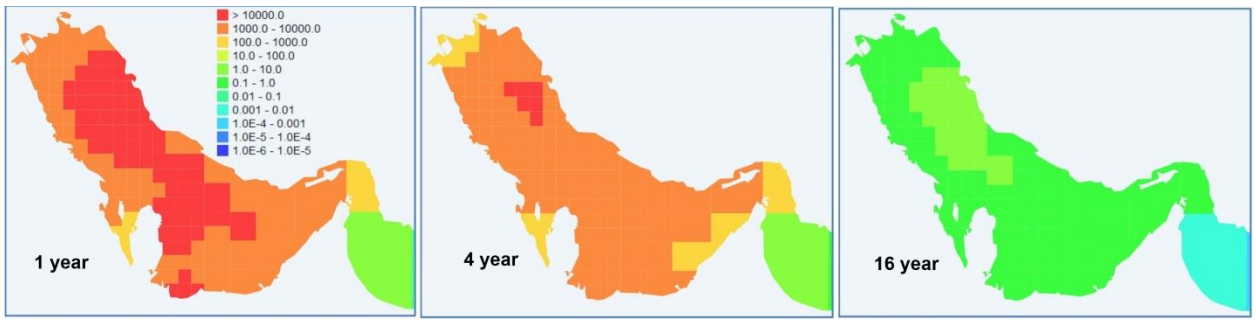


**Figure S15**. Distribution of the $^{106}Ru$ concentration in the upper layer of sediment (Bq kg$^{-1}$) at the Arabian Gulf surface after deposition for the hypothetical accident scenario at Barakah NPP.

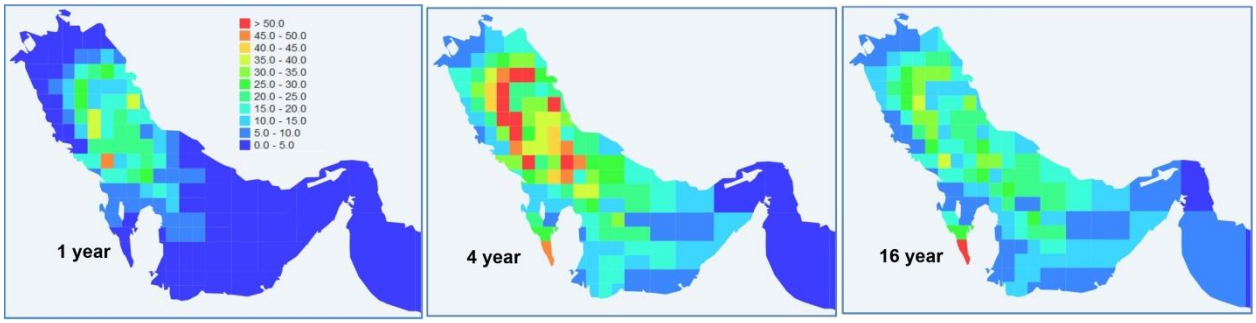


**Figure S16.** Distribution of the $^{90}Sr$ concentration in the upper layer of sediment (Bq kg$^{-1}$) at the Arabian Gulf surface after deposition for the hypothetical accident scenario at Barakah NPP.